Low-RPM torque converter (LRTC) with integrated direct shaft flywheels

D. Salar, E. Hultman and A. Savin

Abstract—The low-RPM Torque Converter (LRTC) is a rotating generator for use on the seabed with the wave motion on the sea surface as the driving force. The concept consists of two identical generators connected through a spring drum with a built-in ball bearing clutch. The drum connects to a buoy on the sea surface via a wire rolled around the spring drum. Sea waves cause the buoy to move upwards or downwards and pull the wire in either direction. This movement causes the generators to spin.

This article presents an upgrade of the LRTC generator and an upgraded hardware and software measurement system. We designed a thin-disc flywheel for direct connection to the generator's rotor shaft as well as an electronic measuring system for more accurate measurements and less disturbances. This article examines three experiments. The first two experiments investigate the performance of the flywheels and compare the performance of the LRTC system with and without the flywheels. The third experiment investigates the optimization of the flywheel mass by increasing its mass with thin discs.

A six-joint industrial robot simulated all movements. The robot simulated several sinusoidal types of wave motions with different time periods as well as real wave climate conditions. The experiments show that the addition of flywheels to the LRTC system increases both peak power and average output power in addition to softening the output power oscillation.

Keywords— **LRTC; Flywheel; Robot; Generator; Wave energy; Renewable energy.**

I. INTRODUCTION

THE discussion about energy use and energy sources has become a global topic, as has the concern about the environment and environmentally friendly services.

Fossil energy sources have a negative effect on the environment. Replacing fossil energy sources with environmentally friendly energy sources continues to gain importance. Renewable energy is a successful breakthrough from both an environmental and an economic perspective [1]. There are different ways to capture energy from natural sources such as wind and ocean waves.

The latter are one of the most attractive sources of energy today. Ocean waves are abundant and waves are generated continuously regardless of the time of day or season of the year. Hence, ocean waves have a high utilization factor and a high energy density [2].

There are already many wave energy converters in the world but sustainable and inexpensive electricity generation remains a challenging goal for many researchers and electricity suppliers [3][4][5].

Renewable energy generation has been an important topic at Uppsala University for many years. There have been several research projects on renewable energy sources and some of them became end products such as the Uppsala University Wave Energy Converter (UU-WEC) developed by the Lysekil project, (see Fig. 1).

The UU-WEC is a linear direct-drive generator connected to a point-absorber. Uppsala University developed this concept in collaboration with the Seabased AB Company. Site tests were carried out in Lysekil on the Swedish west coast. For several years, the Lysekil project has developed and increased the efficiency of the WEC and the transmission of the generated power [6] [7] [8].

In recent years, Uppsala University started a new renewable energy concept, the Low RPM Torque Converter (LRTC) [9]. The LRTC is a rotating electric generator that converts ocean wave motions into a mechanical motion leading to the generation of an electric current. The concept is similar to the UU-WEC in its motion transformation, i.e. the LRTC is placed on the seabed and a point absorber, a buoy, on the sea surface connects to the LRTC via a wire.

In this project, we investigate a direct shaft flywheel integration to the LRTC and its effect on the generated output power. We designed a flywheel for this concept and constructed a printed circuit board (PCB) measuring

Manuscript submitted 2 July 2022; revised 14 December 2022, published 31 March 2023. This is an open access article distributed under the terms of the Creative Commons Attribution 4.0 licence (CC BY http://creativecommons.org/licenses/by/4.0/). Unrestricted use (including commercial), distribution and reproduction is permitted provided that credit is given to the original author(s) of the work, including a URI or hyperlink to the work, this public license and a copyright notice. This article has been subject to single-blind peer review by a minimum of two reviewers.

This work was financially supported by Carl Tryggers Stiftelse, Stockholm (Project nr. CTS 16: 404), Standup for Energy and Uppsala University.

Dana Salar (corresponding author), Erik Hultman and Andrej Savin are at the Department of Electrical Engineering, (Division of Electricity), Uppsala University, Box 534, 7512 Uppsala, Sweden (e-mails: dana.salar@angstrom.uu.se, erik.hultman@angstrom.uu.se and andrej.savin@angstrom.uu.se)

Digital Object Identifier: https://doi.org/10.36688/imej.6.1-10

system. An industrial six-joint robot simulated the wave motion. We constructed a measuring system for experimental evaluation using the industrial robot as a wave motion emulator.

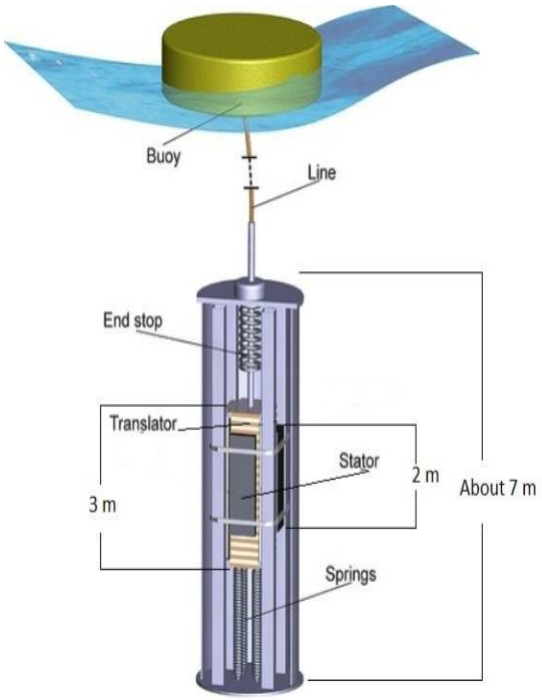

Fig. 1. UU-WEC, developed at Uppsala University

II. LRTC CONCEPT

The LRTC concept consist of two rotating generators. The rotating shaft (rotor) from each generator is placed opposite the other and they are connected by a wire drum. The wire drum has two built-in shaft clutches in the form of ball-bearings.

The shaft clutch allows rotation in one direction only, i.e. the generators spin in opposite directions (see Fig. 2A).

The wire drum connects to the point absorber on the sea surface via a wire to which pulls the drum when the sea waves pick up the buoy. Furthermore, the wire drum is connected to a constant force power spring that pulls the drum in the opposite direction when the traction from the buoy decreases (see Fig. 2B).

When sea waves lift the buoy, the wire is pulled causing the wire drum to rotate in one direction, which pulls generator no. 1 in the same direction as the drum [9]. When the sea waves fall and the traction from the buoy decreases, the spring pulls around the drum and pulls generator no. 2 in the opposite direction to generator no. 1.

In this article, we are investigating the effect of adding flywheels to the LRTC. Each of the generators has a flywheel connected at the back end of the rotor shafts (see Fig. 3).

The flywheel's task is to store the energy, to increase the output power and to reduce the ripple amplitude for

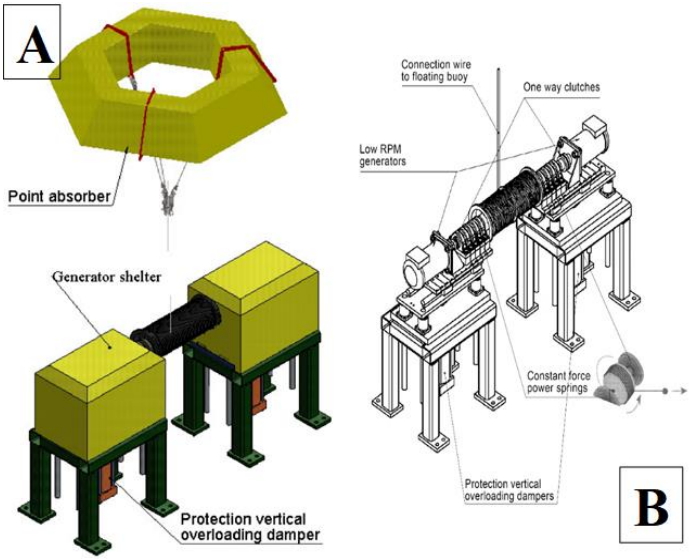

Fig. 2. Generator concept, [9]

a softer output power. The stored energy can be supplied to the generators when the sea waves' energy decreases. In this way, the generator can keep the reduction of the rotational speed as slow as possible while also increasing the output power.

A. *Difference between the LRTC and the LRTC with flywheels*

In this experiment, the main purpose of the flywheels is to smooth out the speed variations of the shaft rotation caused by the unevenly varied torque supply from the

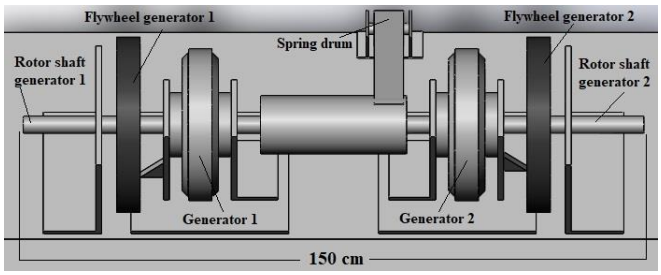

Fig. 3. Experimental generator set-up

sea waves as well as to absorb excess energy.

The generator set-up consists of two 3-phase generators that are connected to each other with a clutch spring drum. The clutch spring drum has an integrated ball bearing clutch at each end that allows movement in one direction only, which results in the generators only spinning in one direction. As the generators are connected in front of each other (see Fig. 3), they can only spin in opposite directions.

B. *Different types of flywheel use*

Different types of technology have been used to control the output power and to store excess energy.

The challenge remains to minimize energy losses both through the output power control system and through energy storage.

Various studies have been carried out to control both output power and energy storage [10] [11] [12].

In these studies, flywheels are used for stabilization and filtration of current/voltage transients of the output power and/or for energy storage. These systems do not have any mechanical connections from the energy source with the generator .

For energy storage purposes, a larger (wider) flywheel system is used which is driven by a motor/generator (M/G) to drive/feed the flywheel system with excess energy (energy storage). The stored energy from the flywheel can then be used through the M/G.

Other technologies use a so-called thin-disk flywheel. This is reminiscent of the above technology as the flywheel system is disconnected mechanically from the generator system.

The generator system from the energy source drives/feeds the flywheel system electrically with absorbed energy. The flywheel system is then used mainly to phase out/smooth the absorbed energy, so the power is filtered to an acceptable output power [13] [14] [15].

In our project, we used a solid thin disk flywheel made of cast iron both to equalize and stabilize the absorbed energy (as a filter) and to store excess energy. The stored energy is utilized to get the maximum power output from the generator system.

The difference between our system and the above-mentioned systems is that the flywheels are connected directly and mechanically (in the same shaft) to the generator.

Using flywheels in this way means that the energy loss is reduced and the output power is increased, yet the design remains simple.

For more energy storage over time, the system can be supplemented with an energy storage system such a battery or a flywheel system for energy storage purposes [10].

Normally, low rpm units are made of cast iron: it is quite inexpensive compared to other materials and has a good energy storage per unit weight.

The most commonly used thin disk flywheel designs are solid, rim, web and arm types [16].

In order to design a flywheel for maximum energy storage efficiency, a flywheel has to be designed specifically for that purpose [17] [18] [19] [20].

C. LRTC flywheel design

Flywheels are used in different areas, in different ways, for different goals and can be manufactured from different kinds of materials. Thus, flywheels can be designed depending on the case and the goal.

The kinetic energy E_k storage in rotating mass is given as:

$$E_k = \frac{1}{2}m(\omega r)^2 = \frac{1}{2}(mr^2)\omega^2 = \frac{1}{2}I\omega^2 \ \ [\mathrm{J}], \quad (1)$$

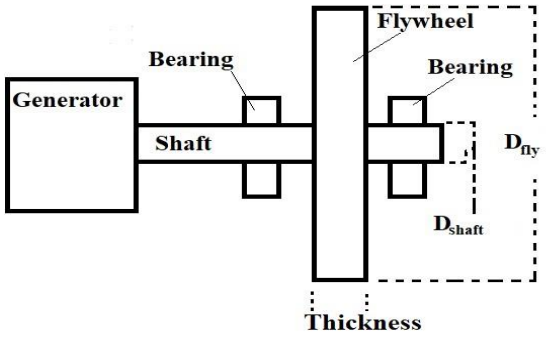

Fig. 4. Flywheel model

where I is the mass moment of inertia, r is radius of the disk and ω is the angular velocity.

$$I = \int x^2 dm_x \quad [kgm^2], \quad (2)$$

where x is the distance from the rotating shaft to the differential mass dm_x.

For solid disk I is given as:

$$I = \frac{1}{2}mr^2\,[kgm^2], \quad (3)$$

where *m* is the mass and r are the radius of the disk.

In our experiment, we have the following data (see Fig. 4):

TABLE I
FLYWHEEL PROPERTIES

Flywheel properties	
Material	Cast Iron
Geometry	Thin disk
Mass	23.5 kg
Velocity	80 RPM
Thickness	4 cm
Diameter flywheel (Dfly)	28 cm
Diameter shaft (Dshaft)	2 cm
Maximum energy storage	8.1 J

In this case (see Table I and Fig. 4), equation (1) and (3) are used to calculate the total kinetic energy stored in the flywheel.

The flywheel properties have been selected according to Table I above based on the robot's payload, the simulated wave speed and the concept set-up size in regard to the desired moment of inertia.

In this experiment, the maximum recommended speed of 80 RPM is used for the generator, which corresponds to 1000 mm/s vertical wire/buoy velocity.

The maximum energy storage achieved in this set-up is 8.1 J. The flywheel was designed for research purposes, to see if it is reasonable to use and what

problems may arise. The set-up was originally built without flywheels and the clutch bearings between the generators and the spring drum were not chosen for adding flywheels. Ideally, the clutch bearings and spring drum should be designed as one unit. The most critical part of this line-up is that the spring drum that pulls generator number 2 is not strong enough (see Fig. 3).

To investigate the flywheel size in detail, we performed additional tests with 10 kg and 20 kg of mass added to each flywheel (see Fig. 5). Due to the limitation of the robot's payload these tests were performed at low speeds.

The flywheels integrated to the LRTC are hereafter referred to as FW, FW+10 and FW+20.

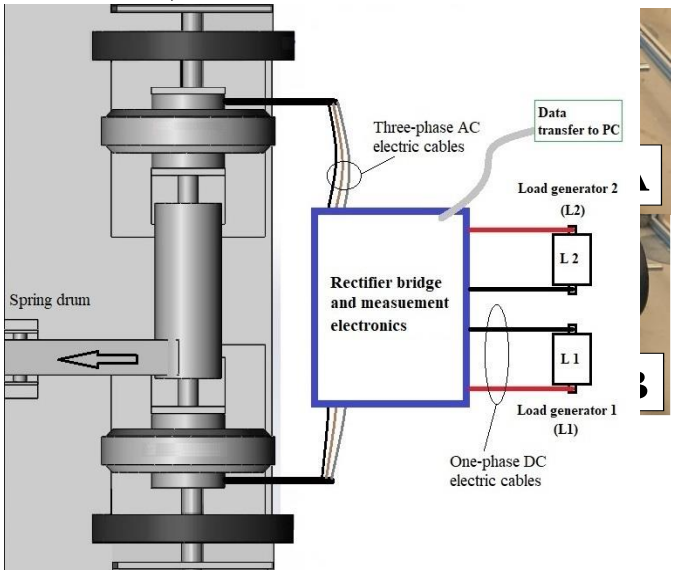

Fig. 7. Experiment set-up

III. EXPERIMENTAL SET-UP

We used an industrial six-joint robot with 6 degrees of freedom (6-DOF) to test the properties and performance of the LRTC by emulating the heaving movement of ocean waves.

In our experiment, we tested different kinds of vertical movements, which for the most part consisted of sinusoidal wave movements with different periods. Several real ocean wave motions, simulated from the field data, were used as well.

The industrial robot is an ABB robot, type IRB6650S. The robot's payload capacity is 200 kg. The robot reaches up to 3 m in length from the robot's base point. With such a robot manipulator, one can simulate different movements, including real wave climates, with high precision [21].

A. Robot cell

The experiments in this article are similar to those previously published for experiments with the LRTC without flywheels [9]. The generator set-up has been upgraded with both flywheels and a reinforced spring drum. In addition, we built a more advanced and more accurate measuring system.

An industrial robot, connected to the generator with a wire to the drum, via a force measurement unit, replaces the point absorbing surface buoy in an actual offshore installation (see Fig. 6A and 6B). On the way up, the robot pulls the wire up and generator 1 spins via the clutch drum. On the way down, the spring, which is connected to the clutch drum, pulls generator 2 in the other direction.

In this way, the generators continuously maintain their movement, each in its own direction, until braked electrically through power outtake and/or mechanically through resistance.

1) *Measurement set-up*

While the generators are spinning, power is

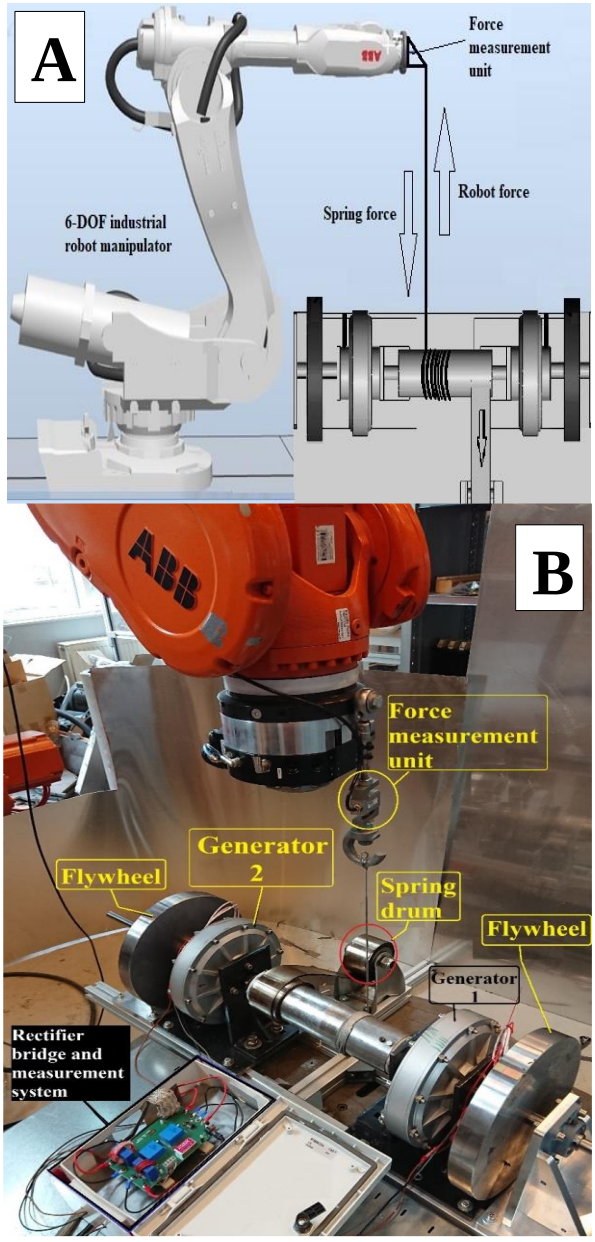

Fig. 6. Experimental set-up

generated. The amount of power depends on the load and the simulated wave speed. In this experiment, we loaded to the maximum load (33 ohms). The generators' three-phase output is connected to an electronics box (see section IV) where the output power is rectified, after

which the voltage and the current are measured to yield the power. Measurement data are sent in real time to a computer to be sorted and logged (see Fig. 7).

B. *Measurement system*

A new measurement system was constructed for measuring the current, the voltage output and the wire traction force in the LRTC during the experiments (see Fig. 8).

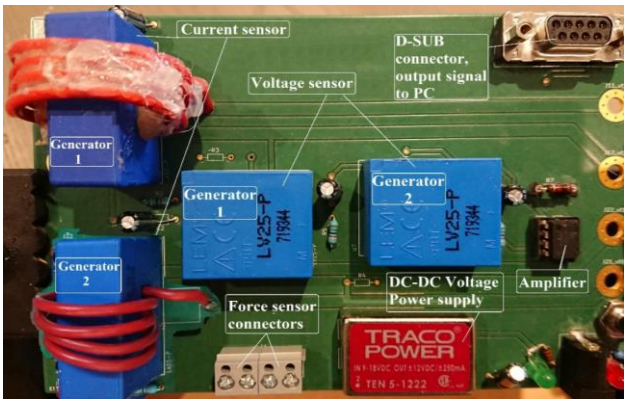

Fig. 8. Measurement board

The PCB measuring unit contains different types of components and sensors depending on the measurement accuracy and signal sensitivity.

The current is measured with a hall-effect sensor of the LEM LA50-P type. We also measured the current for generator 1 and generator 2 (see Fig. 7). The current or power output cable for generator 1 and generator 2 passes through a current sensor 5 times to amplify the current measurement signal, because the current signal is measured in mV.

The voltage is measured across loads 1 and 2 for generators 1 and 2 respectively. For the voltage measurement, a sensor of the LEM LV25-P type is used for each generator (See Fig. 8). This sensor is galvanically insulated to eliminate most interferences.

An 'S' beam force sensor is used to measure the traction force in the wire between the industrial robot and the LRTC (see Fig. 5A and 5B).

The output of the signal from the force sensor requires a signal amplifier and signal processing software. A simple signal amplifier (1:80 times) was implemented in the measurement board for communication with the computer for reading and processing (see Fig. 8).

C. *Experiments*

Several kinds of wave motion experiments were performed for this concept. The first experiment (Exp. I) started with simple sine wave movements with a fixed amplitude and two different time periods [21]. The experiments were performed both with and without flywheels to investigate the impact of the flywheels compared to the concept without flywheels (see Fig. 9, 10, 11 and 12).

- Exp. I.1a: amplitude 300 mm, period time 2 s, LRTC
- Exp. I.1b: amplitude 300 mm, period time 2 s, LRTC with FW
- Exp. I.2a: amplitude 300 mm, period time 4s, LRTC
- Exp. I.2b: amplitude 300 mm, period time 4s, LRTC with FW

The second experiment (Exp. II) was performed by repeating recorded real ocean wave motions. The emulated motions were 120 s selected extractions from the 1200 s recordings, due to the limitation of the generator stroke length of max 750 mm [21]. These were characterized by the following significant wave heights (Hs) and wave energy periods (Te):

- Exp. II.1a: Hs 0.50m, Te 3.98s, LRTC
- Exp. II.1b: Hs 0.50m, Te 3.98s, LRTC with FW
- Exp. II.2a: Hs 0.75m, Te 5.74s, LRTC
- Exp. II.2b: Hs 0.75m, Te 5.74s, LRTC with FW
- Exp. II.3a: Hs 1.00m, Te 4.02s, LRTC
- Exp. II.3b: Hs 1.00m, Te 4.02s, LRTC with FW

The third experiment (Exp. III) was performed with a slower sinusoidal motion with added masses to the flywheels (see Fig. 8):

- Exp. III.a: amplitude 300 mm, period time 4 s, LRTC with FW
- Exp. III.b: amplitude 300 mm, period time 4 s, LRTC with FW+10
- Exp. III.c: amplitude 300 mm, period time 4 s, LRTC with FW+20

IV. RESULTS

The experiments were performed in three parts. The first and second part of the experiments were to detect differences between the LPTC generator with and without flywheels. The third part of the experiments investigated the effect of adding weights to the flywheels.

The results show that the LRTC with FW can perform better and reach its maximum power. The generators were loaded to maximum load, as in the old experiments without flywheels [9] to get the maximum power, while at the same time, the set was tested for the worst-case electrical loads (see Table II).

Fig. 9 is assembled so that it is easier to see the differences between the different test cases, but they are not synchronized in time and neither are Fig. 10 and Fig. 14.

A. *Result Experiment I*

In this experiment (Exp. I.1.a), a fast robot movement was used so the generator set-up could get the maximum output power. We can observe from the result curves (see Fig. 9) that the peak output power of generator 1 is about 200 W, while the peak output power of generator 2 is about 120 W. The fact that the output power of generator 2 is lower than that of generator 1 is because the spring connected to generator 2 cannot apply enough torque to achieve maximum rated output power.

TABLE II
EXP. II RESULT, SINUSOIDAL WAVE MOTION, AMPLITUDE 300 MM

Period time 2 s	**Generator 1 Peak Power Output (W)**	**Generator 2 Peak Power Output (W)**	**Generator 1 Average Power Output(W)**	**Generator 2 Average Power Output (W)**	**LRTC Average Power comparison (%)**
Exp.I.1a	125	121	27	26	100
Exp.I.1b	200	119	58	41	187
Period time 4 s					
Exp.I.2a	32	30	6.8	6.4	100
Exp.I.2b	33	29	8	7.3	116

TABLE III
EXP. II RESULT, REAL OCEAN WAVE MOTION

Real ocean wave motion	**Generator 1 Peak Power Output (W)**	**Generator 2 Peak Power Output (W)**	**Generator 1 Average Power Output (W)**	**Generator 2 Average Power Output (W)**	**LRTC Average Power comparison (%)**
Exp.II.1a	75	61	3.7	3.4	100
Exp.II.1b	78	61	4.2	4.0	114
Exp.II.2a	68	113	4.1	5.3	100
Exp.II.2b	74	113	5.3	7.0	131
Exp.II.3a	220	133	7.5	7.4	100
Exp.II.3b	295	136	10	9	128

TABLE IV
EXP. III RESULT, SINUSOIDAL WAVE MOTION, AMPLITUDE 300 MM

Period time 4 s	**Generator 1 Output Peak Power (W)**	**Generator 2 Output Peak Power (W)**	**Generator 1 Output Average Power (W)**	**Generator 2 Output Average Power (W)**	**LRTC Average Power comparison (%)**
Exp.III.1a	33	29	8	7.3	100
Exp.III.1b	31	28	8.5	8	108
Exp.III.1c	31	29	9	8.7	116

It can be noted (see Fig. 9 and Fig. 10) that the generator set-up with flywheels requires more traction force to spin the generator system. Furthermore, the traction force curve is not in line with the output power curve as it does with the generator set-up without flywheels for both experiments (Exp. I.a and Exp. I.b).

The generator requires more force to start spinning due to the weight of the flywheel. Additionally, the generator starts generating power and the traction forces becomes smoother, only when the flywheel has started to spin.

The clear traction force peaks can be seen in the figures 9 and 10 due to the spring system being wobbly and not having a smooth motion.

The average power for generator 1 with flywheel is 58 W. This fits well with the generator specification which has a rated power output of 60 W. The set-up with flywheels is a clear improvement to the one without flywheels.

The flywheels' contribution is clear in the result: the average power output almost doubles and the output power for both generators never goes to zero.

In a slower motion, Exp. I.1b test results (see Fig. 10) show that the power output for generator 1 and generator 2 is at the same level, about 30 W. This is because the spring which pulls generator 2 is faster than the robot movement. This can also be observed when the lift force curve is between 200 and 750 N with potential in 450 N (sleep mode). The robot is subjected to a force in both directions: while the robot pulls generator 1 up, the lift force curve goes close to 750 N (force from: flywheel + spring + generator 1 load) and on the way down the force goes down close to 200 N (spring force). In the case where the spring and the robot's downwards movement become equal to each other, the lift force should be close to zero.

B. Result Experiment II

In part two of the experiments, data from measured sea wave motions were used. It was interesting to see how the robot and the generator can work together in an almost real buoy movement (see Fig. 11, 12 and 13). In this experiment, we also investigated the differences between the LRTCs with and without flywheels. The results clearly show that the flywheels improve the average output power (see Table III).

C. *Result Experiment III*

Some simpler tests on increasing the weight of the flywheels were done at lower sinusoidal movement speed. We increased the weight by mounting a disk mass to the flywheel shaft of 10 kg and 20 kg (see Fig. 8 A and 8B).

The results showed that with an increase of 10 kg (total mass 33 kg for each generator) to the flywheel, the average power increased by 10 % (see Fig. 14). By increasing the flywheel mass by 20 kg (total mass 43 kg for each generator), the average power increased by 20 % (see Table III).

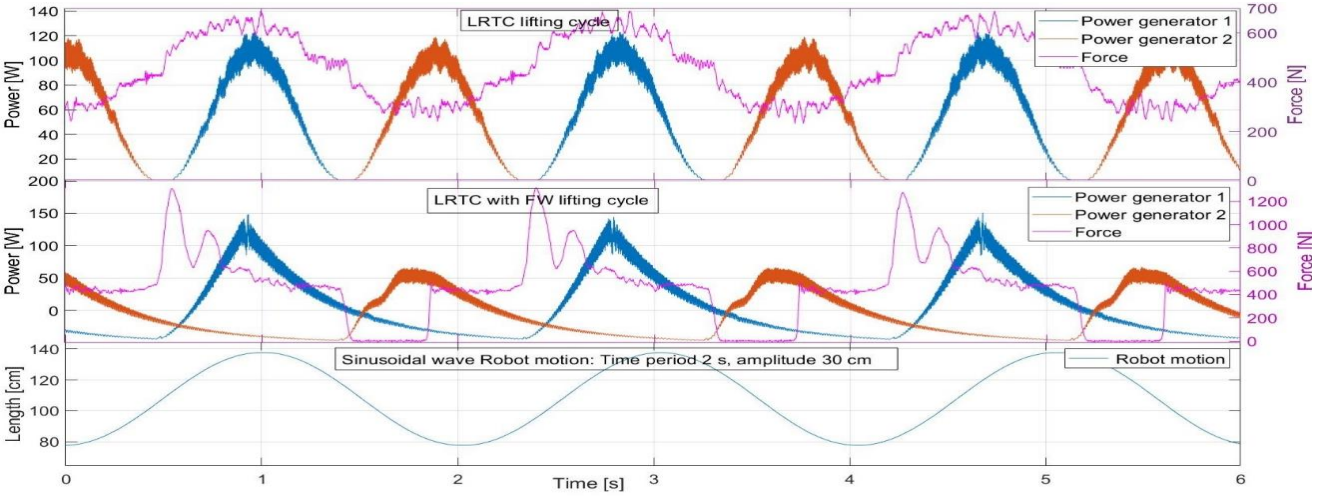

Fig. 9. The LRTC lifting cycle series for Exp. I.1a and Exp. I.1b. Sinusoidal motion with amplitude 300 mm, time period 2 s

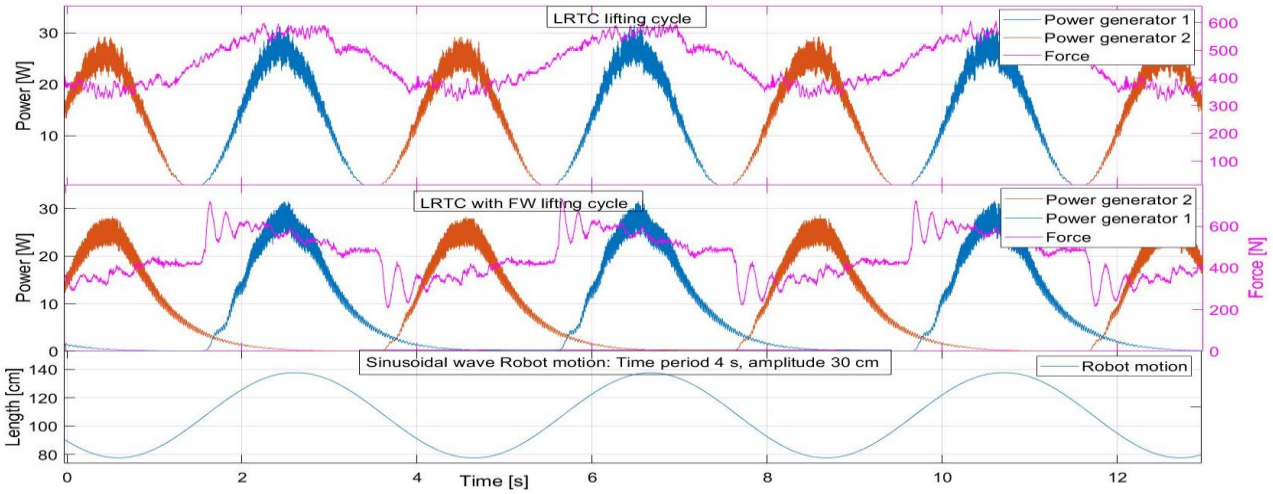

Fig. 10. The LRTC lifting cycle series for Exp. I.2a and Exp. I.2b. Sinusoidal motion with amplitude 300 mm, time period 4 s

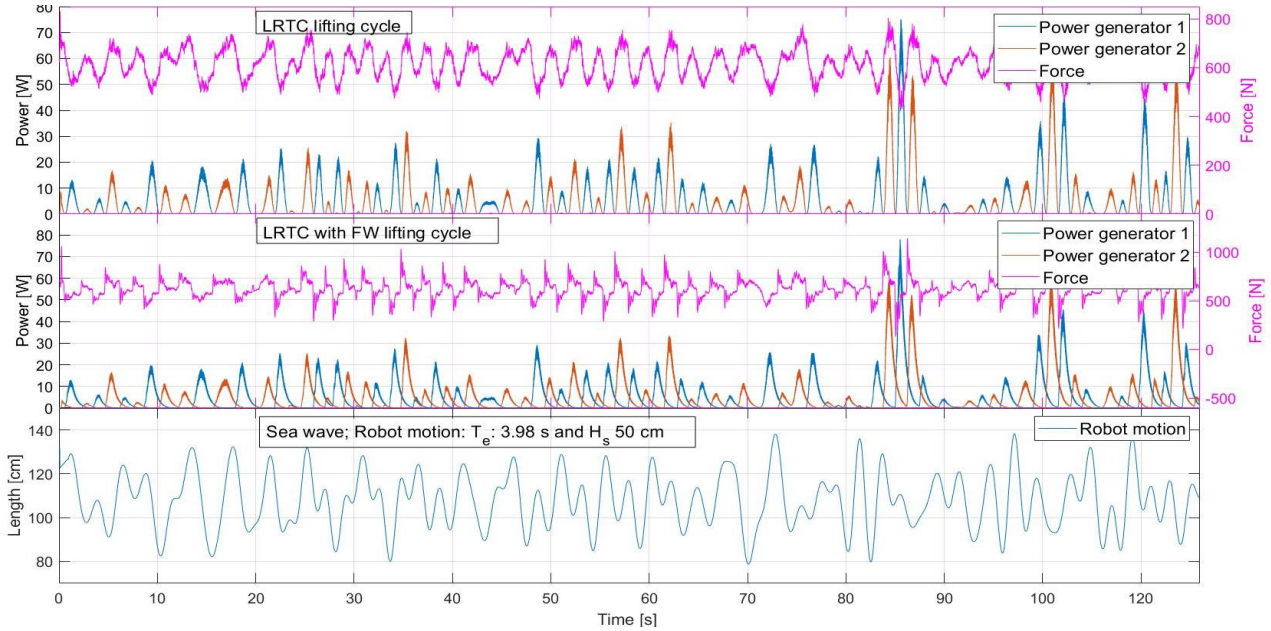

Fig. 11. The LRTC lifting cycle series for Exp. II.1a and 1b. Sea wave motion with Hs = 0.50 m and Te = 3.98 s

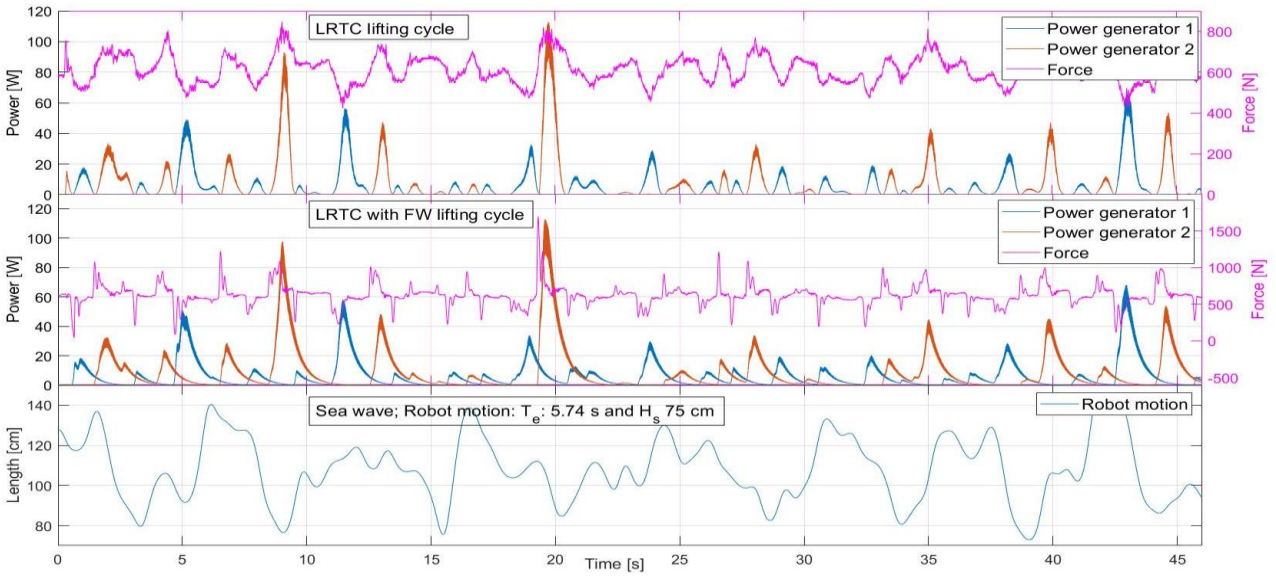

Fig. 12. The LRTC lifting cycle series for Exp. II.2a and 2b. Sea wave motion with Hs = 0.75 m and Te = 5.74 s

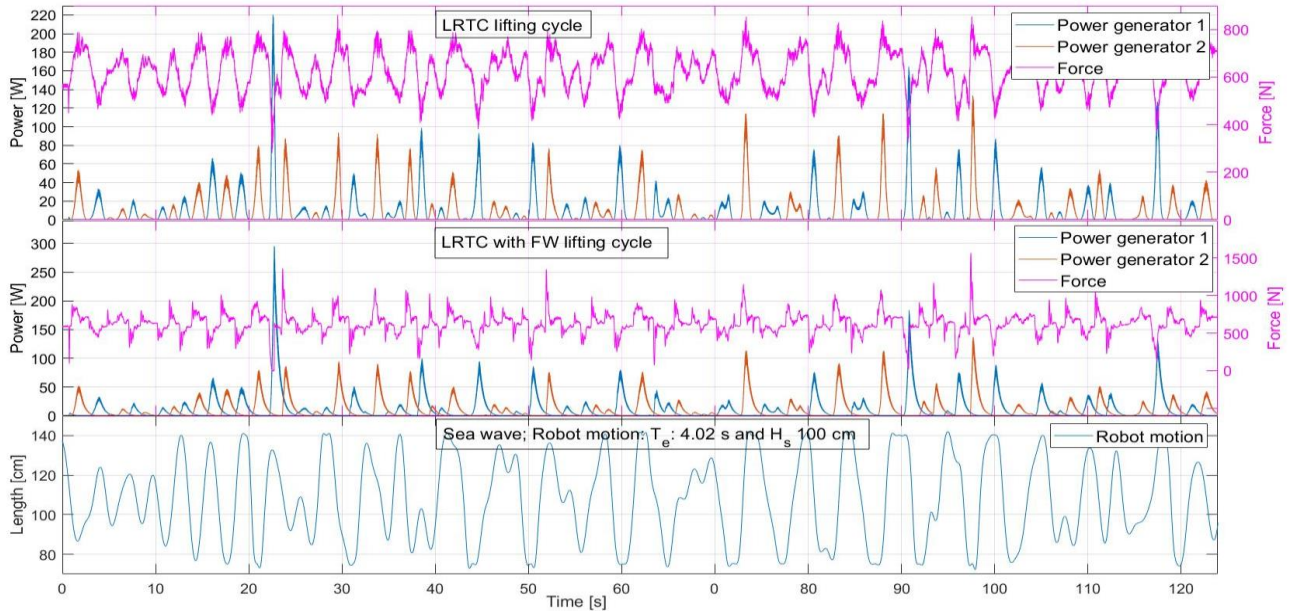

Fig. 13. The LRTC lifting cycle series for Exp. II.3a and 3b. Sea wave motion with Hs = 1.0 m and Te = 4.02 s

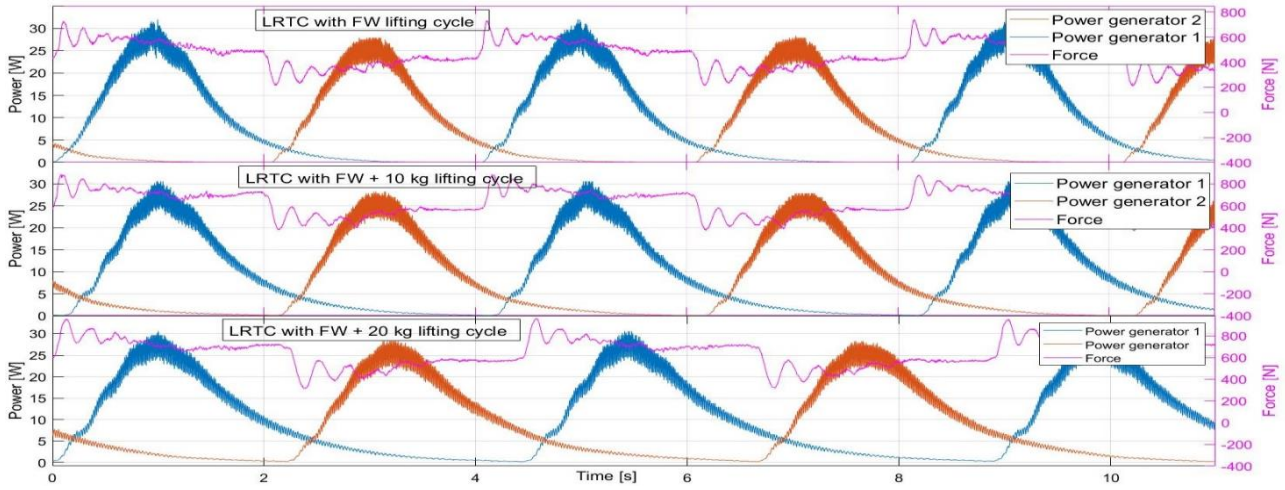

Fig. 14. The LRTC lifting cycle series for Exp. III. a, b and c. Sinusoidal motion with amplitude 300 mm, time period 4 s

V. DISCUSSION

With flywheels connected to the generator, more power is required to spin the generators. In our upgraded set-up, the robot was powerful enough to rotate generator 1, but for generator 2, a more powerful spring was installed.

According to the power measuring unit, the old generator without flywheels in idle position shows 176 N in traction forces in the wire between the generator and the robot. After upgrading with flywheels and a stronger spring, the wire traction force in idle position shows 608 N.

In sleep mode, all traction force comes from the spring drum. The robot's payload comes with a limit of 200 kg. With the experiments for sinusoidal movement, the tensile forces were about 150 kg. For the same movement without flywheels and a weaker spring, the tensile forces were about 50 kg. We avoided snap load forces so the robot could cope with the sinusoidal wave motions, but this is difficult when it comes to wave climate motions.

In the current set-up, the system lacks a hydrodynamic model, which affects the result. A hydrodynamic model implements the simulation of the buoy movement and provides a more accurate output power.

The flywheels were a clear and distinct improvement of the system. The flywheels contributed to a higher peak power output and a higher average power output with a softer output power oscillation. In our tests, the flywheels connected to the LRTC system did not show any disadvantages compared to the LRTC without FW but a higher peak power output can affect the system negatively.

With the flywheel set-up, power set-point tracking can be accessed more easily. The big challenge with reaching power set-point tracking for wave energy is that the power output is very oscillating.

A. *Future works*

The experimental set-up can be divided into two parts, the generator and the robot. It is difficult to upgrade the generator set-up in the future. At present, it has certain shortcomings, such as the fact that the spring drum that pulls generator 2 is too weak.

The flywheels should be a few factors larger to store more energy and contribute to a softer power drop.

Experiment III shows that the flywheels clearly need more mass to boost optimization, since larger and heavier flywheels increase both the peak power output and the average output power as well as providing a softer output power. Due to the robot payload, it is currently not possible to increase the flywheel mass.

For these upgrades and for better measurement accuracy, we recommend a new generator set-up with a higher output power.

For the robot part, in addition to enabling the robot to handle the lifting forces from the new generator set-up, a hydrodynamic model should be implemented in the wave motion simulation. The buoy cannot be seen as a point that moves up and down with sea wave movements, because the buoy has gravity force downwards and traction forces in the wire (connecting the buoy and the generator on the sea bed) which slows the buoy's movement upwards.

Therefore, it is necessary to implement a hydrodynamic model in the simulation system to be able to simulate the buoy movements correctly [22] [23].

To avoid slack in the wire during snap load motion, a vertical overload damper should be implemented in the wire system.

VI. CONCLUSIONS

Research and optimization of an LRTC with FW compared to an LRTC without FW showed a clear advantage of having flywheels in the system.

Experiment (I) shows an increase in both peak power output and average output power as well as output power oscillating damping (see Fig. 9, Fig. 10 and Table II).

In experiment (II), where the experiments were done with data from a real sea wave climate, the results showed an increase in the average power output, while the peak power output remained almost the same (see Fig. 11, Fig. 12 and Table III).

Experiment (III) examined the increase of the flywheels' mass and its effects, by adding two flywheel thin disks in two steps (see Fig. 14 and Table IV).

The experiments that we were able to do with the robot wave emulator system showed a sufficiently positive increase in the average output power to consider the need for further research into the size and mass of the flywheels.

The LRTC concept needs a major upgrade in the future, including larger flywheels. An upgrade of the robot wave emulator system for handling larger forces is needed as well. For even more accurate results a hydrodynamic model needs to be implemented.

VII. ACKNOWLEDGMENTS

The authors are grateful to ABB Corporate Research, for the donation of the robot used in the experiments.

VIII. REFERENCES

[1] Junejo F, Saeed A and Hameed S (2018) Energy Management in Ocean Energy Systems. Comprehensive Energy Systems, VOL.5, pp 778-807, https://doi.org/10.1016/B978-0-12-809597-3.00539-3.

[2] J. Falnes, Ocean Waves and Oscillating Systems: Linear Interactions Including Wave-Energy Extraction. Cambridge: Cambridge University Press, 2002.

[3] Mueller M. and Wallace R (2008), Enabling science and technology for marine renewable energy, Energy Policy, vol. 36, no. 12, pp. 4376-4382

[4] Elwood D, C. Yim S, Prudell J, Stillinger C, von Jouanne A, Brekken T, Brown A, and Paasch R (2010) Design,

construction, and ocean testing of a taut-moored dual-body wave energy converter with a linear generator power take-off. Renewable Energy, Volume 35, pp.348–354.

[5] Dongsheng Q, Rizwan H, Jun Y, Dezhi N, Binbin L (2020) Review of Wave Energy Converter and Design of Mooring System. Sustainability, 12(19), 8251.

[6] Leijon M, Bernhoff H, Ågren O, Isberg J, Sundberg J, Berg M, Karlsson K E, and Wolfbrandt A (2005) Multiphysics simulation of wave energy to electric energy conversion by permanent magnet linear generator. IEEE transactions of energy conversion, Vol.20, No.1, pp.219–224.

[7] Leijon M, Boström C, Danielsson D, Gustafsson S, Haikonen K, Langhamer O, Stromstedt E, Stålberg M, Sundberg J, Svensson O, Tyrberg S, and Waters R (2008) Wave energy from the North Sea: Experiences from the Lysekil research site. Surveys in Geophysics, Volume 29, pp.221–240.

[8] Leijon M, Waters R, Rahm M, Svensson O, Boström C, Strömstedt E, Engstrom J, Tyrberg S, Savin A, Gravrakmo H, Bernhoff H, Sundberg J, Isberg J, Agren O, Danielsson O, Eriks-son M, Lejerskog E, Bolund B, Gustafsson S, and Thorburn K (2009) Catch the wave to electricity. IEEE Power and Energy Magazine, Volume 7, Issue 1, pp.50–54.

[9] Tørum A, and Gudmestad O (2012) Wave power absorption as a function of water level and wave height: Theory and experiment. Springer Science and Business Media, VOL. 178.

[10] Savin A, Salar D and Hultman E (2021) Low-RPM Torque Converter (LRTC). Energies, VOLUME 14, NO. 16, ARTICLE NUMBER 5071.

[11] Brenda R-De, Alonso M, Amaris H, and De Santiago J (2019) Wave Power Output Smoothing through the Use of a High-Speed Kinetic Buffer. Energies 12, no. 11: 2196. https://doi.org/10.3390/en12112196

[12] Cardenas R, Pena R, Asher G and Clare J (2001) Control strategies for enhanced power smoothing in wind energy systems using a flywheel driven by a vector-controlled induction machine. Industrial Electronics IEEE Transactions on, vol. 48, no. 3, pp. 625-635.

[13] Wang L, Chun-Yu L and V. Prokhorov A (2017) Stability analysis of a microgrid system with a hybrid offshore wind and ocean energy farm fed to a power grid through an HVDC link. Industry Applications Society Annual Meeting IEEE, pp. 1-9.

[14] Gostavo O. Guarniz A, Milad Sand Segen F. E(2021) Application of the Latching Control System on the Power Performance of a Wave Energy Converter Characterized by Gearbox, Flywheel, and Electrical Generator. J. Marine. Sci. Appl. 20, 767–786. https://doi.org/10.1007/s11804-021-00238-7.

[15] Qiaofeng L, Xiaofan L, Jia M, Boxi J, Shui C and Lei Z (2021) Tunable Wave Energy Converter Using Variable Inertia Flywheel," in IEEE Transactions on Sustainable Energy, vol. 12, no. 2, pp. 1265-1274, doi: 10.1109/TSTE.2020.3041664.

[16] Yiqing Y, Peihao C and Qiang L (2021) A wave energy harvester based on coaxial mechanical motion rectifier and variable inertia flywheel, Applied Energy, Volume 302, 117528, ISSN 0306-2619, https://doi.org/10.1016/j.apenergy.2021.117528.

[17] Kale V, and Secanell M, (2018) A comparative study between optimal metal and composite rotors for flywheel energy storage systems. ScienceDirect, VOL.4, pp.576-585.

[18] Amiryar M.E, Pullen K.R, Nankoo D (2018) Development of a High-Fidelity Model for an Electrically Driven Energy Storage Flywheel Suitable for Small Scale Residential Applications. Appl. Sci. 8, 453. https://doi.org/10.3390/app8030453

[19] Hearn E.J (1997) Mechanics of Materials 2. In: Rings discs and Cylinders subjected to Rotation and Thermal Gradients, 3rd edn, Butterworth-Heinemann, pp 117-140. https://docplayer.net/20962407-Rings-discs-and-cylinders-subjected-to-rotation-and-thermal-gradients.html.

[20] Dagnæs-Hansen N. A, and Santos I. F (2018) Magnetically suspended flywheel in gimbal mount - Nonlinear modelling and simulation. Journal of Sound and Vibration, 432, 327-350. https://doi.org/10.1016/j.jsv.2018.06.033.

[21] Hassan S. U, He B and Khayyam U (2019) Design and Analysis of Flywheel for Small Scale Energy Storage System using Different Structures and their Comparison. 4th International Conference on Power and Renewable Energy (ICPRE), pp. 295-299, doi:10.1109/ICPRE48497.2019.9034862.

[22] Hultman E (2022) A robotized dry test rig for wave power. Under revision with Sustainable Energy Technologies and Assessments.

[23] Eriksson M, Isberg J and Leijon M (2005) Hydrodynamic modelling of a direct drive wave energy converter. International Journal of Engineering Science 43, 1377-1387.

[24] Eriksson M, Waters R, Svensson O, Isberg J and Leijon M (2007) Wave power absorption: Experiments in open sea and simulation. J. Appl. Phys., vol. 102.